Geoderma 470 (2026) 117836

Contents lists available at ScienceDirect

Geoderma

journal homepage: www.elsevier.com/locate/geoderma

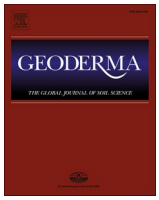

Atlantic Forest conversion to organic banana agroforestry changes soil organic matter composition but not carbon stocks in Brazil

Otávio dos Anjos Leal [a,*], José María De la Rosa [b], Nicolas Brüggemann [a], Holger Wissel [a], Cledimar Rogério Lourenzi [c], Thairine Evaldt Justo [d], Águeda Sánchez-Martín [b], Deborah Dick [e], José António González-Pérez [b], Heike Knicker [f]

[a] Institute of Bio- and Geosciences—Agrosphere (IBG-3), Forschungszentrum Jülich GmbH, Wilhelm-Johnen-Straße, 52428 Jülich, Germany
[b] Instituto de Recursos Naturales y Agrobiología de Sevilla, Consejo Superior de Investigaciones Científicas (IRNAS-CSIC), Avenida Reina Mercedes 10, 41012 Sevilla, Spain
[c] Department of Rural Engineering, Federal University of Santa Catarina (UFSC), Florianópolis 88034-000, Brazil
[d] Catarinense Federal Institute (IFC), R. das Rosas, 88965-000 Santa Rosa do Sul, Brazil
[e] Instituto de Química, Universidade Federal do Rio Grande do Sul, Av. Bento Gonçalves, 7712, Porto Alegre 91501-970, Brazil
[f] Instituto de la Grasa, Consejo Superior de Investigaciones Científicas (IG-CSIC), Campus de la Universidad Pablo de Olavide, Edificio 46, Ctra. de Utrera, km 1, 41013 Seville, Spain

ARTICLE INFO

Handling Editor: Dr. C. Mueller

Keywords:
^{13}C NMR indexes
Thermogravimetry
Lipid proxy
PCA
Nitrogen
Long-term

ABSTRACT

Global population growth will demand a 70% increase in food production by 2050, which may mostly occur in developing countries. In Brazil, organic agriculture expanded notably since the implementation of the National Policy for Agroecology and Organic Production in 2012. In southern Brazil, conventional and organic banana agroforestry systems are expanding quickly over Atlantic Forest, posing increasing pressure on this native biome. Organic farming depends on the multifunctionality of soil organic matter (SOM), which is highly sensitive to land-use change. However, shifts in SOM composition and soil organic carbon (SOC) stocks following Atlantic Forest-to-banana conversion remain largely unacknowledged. We analyzed SOC stocks and SOM composition (0–10 and 10–20 cm layer) using advanced techniques (^{13}C NMR, thermogravimetry, lipid biomarkers) after 18 years of Atlantic Forest conversion to banana in conventional (Banana) and organic agroforestry (Forest + Banana) systems in southern Brazil. We hypothesized: SOC stocks would be similar in Forest and Forest + Banana, but lower in Banana (H1), and that SOM chemical composition in Banana site would contrast more remarkably with that in Forest compared to the Forest + Banana site (H2). SOC stocks were statistically similar across the systems at 0–10 cm (30.6–38.6 Mg ha^{-1}) and 10–20 cm layer (16.1–20.0 Mg ha^{-1}), contradicting H1. However, Banana promoted a marked depletion of labile SOM (O-alkyl C), accompanied by a relative enrichment of more stable compounds (mainly aryl C at 0–10 cm and alkyl C at 0–20 cm). Lower lipid Carbon Preference Index indicated comparatively more degraded SOM in Banana soil (0–20 cm). Overall, SOM aromaticity, hydrophobicity, and thermal stability gradually increased with land-use intensity (Banana > Forest + Banana > Forest), supporting H2.

1. Introduction

The global population reached 8.2 billion in 2024 and is expected to continue growing in the next decades, peaking at around 10.3 billion by the mid-2080s, with most of this growth occurring in developing countries such as Brazil (United Nations, 2013; 2024; FAO, 2025). Meeting food demand will require a 70% increase in global food production between 2005 and 2050, 90% of which is expected in emerging economies (FAO, 2009). Meanwhile, demand for organic food is increasing rapidly. Between 1999 and 2023, the global area under organic agriculture grew from 11 to 99 million hectares, the number of organic farmers reached 4.3 million, and the global organic market was estimated at 136.4 billion euros (FiBL and IFOAM, 2025). In 2023, banana (*Musa* spp.) was the leading organic commodity in Europe and United States (FiBL and IFOAM, 2025).

In Brazil, organic farming has expanded largely since the National

* Corresponding author.
E-mail address: o.dos.anjos.leal@fz-juelich.de (O.A. Leal).

https://doi.org/10.1016/j.geoderma.2026.117836
Received 8 December 2025; Received in revised form 9 March 2026; Accepted 27 April 2026
Available online 16 May 2026

Policy for Agroecology and Organic Production (Presidential Decree No. 7,794, 2012). Between 2013 and 2023, the number of certified organic producers in Brazil increased by 98%, reaching 24,853 farmers, and the area used for organic production increased by 42%, reaching 1.0 million hectares (FiBL and IFOAM, 2015; 2025). Along with other Latin American countries, Brazil plays a strategic role in the global organic market due to its large-scale, export-oriented agriculture, with bananas, coffee, and soybeans among the main organic exports. Among tropical and subtropical fruits, banana leads the global area (27.4%) under organic cultivation (FiBL and IFOAM, 2025).

The rapid expansion of agriculture in Brazil occurs within a broader global context of increasing pressure on soil resources. The fact that one third of soils globally are degraded and losing productivity (FAO and ITPS, 2015) intensifies pressure on natural environments, which often exhibit inherent soil fertility. Thus, agricultural intensification and expansion must be reconciled with environmental preservation. The Atlantic Forest, the predominant natural vegetation at the southern coast of Brazil, has been also under pressure by agricultural expansion (Carlucci et al., 2021).

Recent high-resolution estimates suggest that 28% of the Atlantic Forest cover remains, which is considerably higher than previous estimations, i.e., 11.4–16.0% (Ribeiro et al., 2009), indicating a regenerative power of the forest (Rezende et al., 2018). Nevertheless, the integrity of the remaining Atlantic Forest fragments is continuously at risk, for example due to recent changes in legislation that may simplify environmental licensing processes in the country (Weidlich et al., 2025). Consequently, fragmentation of the Atlantic Forest may continue, with banana cultivation being one of the main activities replacing Atlantic Forest in southern Brazil (Rossato et al., 2025). This region is the smallest of the five regions of the country but accounted for 11% of the national banana area in 2023 (456,522 ha) (IBGE, 2025).

Since the early 1990s, southern Brazil has become a hotspot for organic banana cultivation integrated with Atlantic Forest. Gonçalves (2008) found greater socio-economic gains for these agroforestry farmers compared to conventional banana cultivation, while maintaining tree biodiversity comparable to that in adjacent forest fragments. According to the latest available survey, about 300 farmers produce banana under such organic agroforestry system in the region of Torres city, Rio Grande do Sul State, Brazil (Gonçalves and Motter, 2015).

A central component for maintenance of soil productivity, particularly in organic farming, is soil organic matter (SOM), which is composed of about 58% of carbon (C) (Stockmann et al., 2013). These systems rely primarily on organic fertilizers, minimal soil interventions, and nutrient cycling from crops and forest plants. Thus, the multifunctional role of SOM in maintaining soil fertility, is crucial for ensuring banana yields and the sustainability of the system. Soil organic C (SOC) and total nitrogen (TN) stocks as well as SOM chemical composition are highly sensitive indicators of land use change and management practices (USDA, 2015; Sá et al., 2018). Losses of SOC stocks following forest conversion to agricultural land undermine efforts to increase SOC for climate mitigation (Wei et al., 2014; Beillouin et al., 2023).

Quartucci et al. (2023) examined SOC stock changes (0–20 cm layer) after reforestation (16 years), natural regeneration (17 years), conventional agriculture (25 years) and agroforestry (5.7 and 19-year) following Atlantic Forest deforestation. The authors found that only natural regeneration and long-term agroforestry reached SOC levels comparable to secondary forest (70.4 Mg ha^{-1}). These data are challenged by Ramos et al. (2025), who observed equivalent SOC contents (21.3–22.1 g kg^{-1}, 0–10 cm layer) in southeastern Atlantic Forest compared to an eight-year agroforestry system including intercropping of banana and other species. Contrastingly, Santos et al. (2019) reported a 15 Mg ha^{-1} (0–30 cm layer) increase in SOC stocks 15 years after Atlantic Forest conversion to *Brachiaria* pasture. Overall, Villela et al. (2026) recently reported that the deficit of SOC stocks (0–30 cm layer) in agricultural land previously under native vegetation across Brazil's six biomes (Amazon, Cerrado, Pantanal, Caatinga, Atlantic Forest, Pampa) is largest in Atlantic Forest.

Although several studies emphasize the importance of monitoring SOC changes after Atlantic Forest conversion, differences in cultivation systems hinder the identification of consistent SOC trends. In addition, research has focused mainly in southeastern and northeastern Brazil, where predominantly tropical conditions drive SOC dynamics that differ from subtropical regions (Dieckow et al., 2009; Freitas et al., 2024). Furthermore, the impacts of conventional and organic banana agroforestry systems on SOC stocks after Atlantic Forest conversion remain largely unstudied, despite the spatial and economic representativeness of these areas along Brazil's southern coast. Moreover, the effects of such land-use changes on SOM structure, chemical composition and stability remain unknown, increasing uncertainty about the long-term preservation of SOC stocks (Almendros and González-Pérez, 2025). Teixeira et al. (2024) found that conversion of subtropical Atlantic Forest to managed land altered the interplay between microbial community structure and SOC stocks, with implications for SOM composition and stability. Accordingly, Bieluczyk et al. (2023) reported that management of former Atlantic Forest soils increased SOM humification indexes, indicating the lack of labile SOM associated with lower input of fresh biomass in the managed compared to the forest site.

This study aimed to bring insights into how Atlantic Forest conversion to conventional and organic banana agroforestry systems alters SOC and TN stocks, as well as SOM chemical composition and stability. We combined advanced analytical techniques, such as solid-state cross-polarization magic angle spinning (CPMAS) ^{13}C nuclear magnetic resonance spectroscopy (^{13}C NMR), thermogravimetric analysis (TG), and molecular biomarker profiling of free lipids. Solid-state ^{13}C NMR informs on the chemical nature of SOM, distinguishing between alkyl, O-alkyl, aromatic, and carbonyl C groups (Knicker, 2011), providing insights into SOM transformation processes and the relative contributions of plant- and microbially-derived inputs (Chukov et al., 2018). Soil TG analysis complements this by informing on SOM thermal stability and distinguishing labile and recalcitrant fractions (Plante et al., 2009; De la Rosa and Knicker, 2011; Prats et al., 2021). Free lipid biomarkers, particularly *n*-alkanes, provide additional molecular-level information on SOM sources and diagenetic status, with the Carbon Preference Index (CPI) and Average Chain Length (ACL) serving as recognized indicators (Thomas et al., 2021).

We hypothesize that 1) SOC and TN stocks in the organic banana agroforestry system would be comparable to the Atlantic Forest reference, while lower in the conventional banana site; 2) SOM structural changes would be more pronounced in the conventional banana system, whereas SOM in the organic banana agroforestry system would retain characteristics closer to the Atlantic Forest soil.

2. Material and methods

2.1. Study site location and characterization

The studied sites are located in the municipality of Três Cachoeiras, 27 km south of the city of Torres, Rio Grande do Sul, southern Brazil. The climate is humid subtropical (Cfa) with hot and humid summers, mild winters and year-round precipitation according to Köppen's classification (Alvares et al., 2013). The annual average temperature is 19.8 °C, monthly precipitation is 181 mm, and elevation above sea level is 16 m.

The soil samples were collected at three sites adjacent to each other: Atlantic Forest (Fo), organic banana plantation integrated with Atlantic Forest (Fo + Ba), and conventional banana plantation (Ba) (Fig. S1). The size of Fo, Fo + Ba and Ba areas was 0.5, 2.3 and 2.0 ha, respectively. Both Ba and Fo + Ba areas had been converted from Atlantic Forest 18 years before the realization of this study. The approximate spacing

Table 1
Soil pH, sand, silt and clay content, bulk density (Bd), total porosity (Tp), and water-holding capacity (WHC) in the 0–10 and 10–20 cm layer in the forest (Fo), organic banana agroforestry (Fo + Ba), and conventional banana (Ba) site. Values are means followed by standard deviation within parentheses (n = 3).

Site	Layer (cm)	pH	Sand	Silt	Clay	Bd	Tp	WHC
			g kg^{-1}			g cm^{-3}	cm^3 cm^{-3}	g 100 g^{-1}
Fo	0–10	5.6 (0.3)	331 (30)	353 (25)	316 (12)	0.96 (0.1)	0.64 (0.0)	76.6 (7.4)
Fo + Ba	0–10	6.0 (0.4)	277 (56)	335 (39)	388 (28)	1.06 (0.0)	0.60 (0.0)	79.0 (6.2)
Ba	0–10	5.8 (0.1)	265 (31)	381 (67)	353 (36)	0.95 (0.1)	0.64 (0.0)	89.7 (5.1)
Fo	10–20	5.0 (0.5)	298 (14)	317 (28)	386 (37)	1.04 (0.1)	0.61 (0.0)	74.6 (4.7)
Fo + Ba	10–20	5.1 (0.2)	254 (12)	415 (134)	331 (122)	1.02 (0.0)	0.64 (0.0)	74.3 (4.0)
Ba	10–20	5.6 (0.5)	238 (66)	365 (18)	396 (73)	0.99 (0.1)	0.63 (0.0)	78.6 (1.6)

between banana plants at Ba site was 3 m × 2.2 m, whereas in Fo + Ba site it was 3 m × 2 m. The three areas had the same soil type, a Nitisol (IUSS Working Group WRB, 2015) corresponding to a *Nitossolo Vermelho* according to the Brazilian Soil Classification System of Embrapa (Santos et al., 2018).

The fertilization in Ba area followed the Liming and Fertilization Manual for the States of Santa Catarina and Rio Grande do Sul (CQFS, 2016). Thus, NPK fertilization is based on soil analysis and orchard development stage (pre-planting, growth stage, and maintenance fertilization). In pre-planting stage, on average 130 kg P_2O_5 ha^{-1} and 60 kg K_2O ha^{-1} is applied. In growth stage, 200 kg N ha^{-1} is applied (for intermediate SOM content as in Ba). In the maintenance fertilization stage, 3.0 to 5.0 kg N ha^{-1} $year^{-1}$, 1.0 kg P_2O_5 ha^{-1} $year^{-1}$, and 13 kg K_2O ha^{-1} $year^{-1}$ is applied per estimated ton of banana to be harvested. In Ba site, mostly chemical fertilizers are used, infected banana residues are removed from the area and chemical weeding with glyphosate is performed at beginning and end of summer.

The fertilization in Fo + Ba area was conducted according to recommendations of a local farmers' association (Gonçalves and Motter, 2015) because the aforementioned fertilization manual for conventional banana does not include recommendations for organic banana agroforestry systems. According to the farmer, the levels of NPK applied in Ba are used as reference for banana fertilization in Fo + Ba. However, instead of chemical fertilizers, bokashi compost, manure, and rock powder are used. The specific amount and composition of these products vary from one year to the other, as usually these are produced artisanally, or donated by local companies in the case of rock powder. In Fo + Ba, weeding is conducted manually at beginning and end of summer, and infected banana residues are removed from the field, as similarly performed in Ba site. According to the farmer, soil mechanization (e.g., ploughing and harrowing) in Fo + Ba and Ba has never been conducted until soil sampling for our study.

Given these considerations, we assumed that differences in the investigated response variables were intrinsic of the native (Fo) or cultivation systems (Ba and Fo + Ba) because all three areas were located adjacent to each other, had the same soil type and texture, climate classification, and soil samples were taken at same relief position.

The five main tree species at the Fo + Ba site were: juçara palm (*Euterpe edulis*), jerivá (*Syagrus romanzoffiana*), guava (*Psidium guajava*), embaúba (*Cecropia* sp.) and cedro (*Cedrela fissilis*). In Fo + Ba site, about 150 juçara palm plants and other 45 trees, all native species, were present. These trees are spatially randomly distributed as they are not planted by the farmer but inherited from the forest or have grown spontaneously. At the Fo site, the five main tree species were: juçara palm (*Euterpe edulis*), yellow cinnamon (*Nectandra lanceolata*), capororoca (*Myrsine umbellata*), japan grape (*Hovenia dulcis*) and licurana (*Hyeronima alchorneoides*). The number of trees at Fo site was estimated at 600. Based on this, it is estimated that the number of trees ha^{-1} in Fo (1200) is about 14-fold greater than in Fo + Ba, with relatively minor differences on tree species diversity expected. In a study with eight organic banana agroforestry farms conducted in the same region, Gonçalves (2008) found on average 118 tree species belonging to 37 families in the agroforestry sites, which was very similar to the numbers found in the Atlantic Forest reference sites (114 tree species belonging to 44 families).

2.2. Soil sampling and analyses

Disturbed and undisturbed soil samples were collected (three replicates per site) at the 0–10 and 10–20 cm layer. The geolocation of soil sampling points is displayed in Table S1. The disturbed soil samples were air-dried and passed through a 2-mm sieve for analysis of soil pH, sand, silt and clay content. The undisturbed soil samples were collected with volumetric rings (143.7 cm^3) from the 0–10 and 10–20 cm layers and used for determination of soil total porosity, water-holding capacity, and bulk density, which is required for SOC and N stocks calculation. These analyses were conducted according to Teixeira et al. (2017) for soil characterization (Table 1).

2.2.1. SOC and TN content determination and stocks calculation

For SOC and TN content determination, soil samples were combusted at 1040 °C in an elemental analyzer coupled to an isotope ratio mass spectrometer (EA-IRMS, Flash EA 2000 coupled with a Delta V Plus, Thermo Fisher Scientific, Bremen, Germany). The SOC and TN stocks were calculated based on SOC and TN contents, bulk density and thickness of soil layers (Table 1) according to Bernoux et al. (2002).

2.2.2. SOM composition

2.2.2.1. Solid-state ^{13}C-nuclear magnetic resonance (^{13}C NMR) spectroscopy. Prior to analysis, composite soil samples, formed from the three field replicates, were demineralized with 10% HF according to Gonçalves et al. (2003) to improve the sensitivity of the samples to ^{13}C NMR spectroscopy. The samples were milled, homogenized and subsequently placed into 4 mm zirconium rotors with KEL-F caps. The ^{13}C NMR spectra were obtained with a Bruker Avance III HD 400 MHz (Bruker Biospin, Rheinstetten, Germany) by rotating the sample with a speed of 14 kHz. A ramped 1H pulse was used during 1 ms of contact time to avoid Hartmann-Hahn mismatches. The required number of scans ranged from 15,608 to 193,813 across samples. The ^{13}C chemical shifts were calibrated relative to tetramethylsilane (0 ppm) with glycine (COOH at 176.08 ppm).

The contribution of the C-groups to the total ^{13}C signal intensity was calculated with the MestreNova 10 Software (Santiago de Compostela, Spain). For that, the integration of the signal intensity of each C-group was performed and the area of individual chemical regions in the spectra was divided by the total area (100%) and expressed in percentage (Knicker et al., 2013). Five chemical regions were identified in the spectra: 0–45 ppm (alkyl C), 45–60 ppm (N-alkyl C/methoxyl C), 60–110 ppm (O-alkyl C), 110–160 ppm (aryl C) and 160–225 ppm (carboxyl C) (Knicker et al., 2013). The intensity of the spinning side bands was added to that determined for the chemical shift region between 90 and 160 ppm according to Knicker et al. (2005).

The ^{13}C NMR aromaticity index (ArI) was calculated as the aryl C to alkyl C ratio according to De la Rosa et al. (2018), the hydrophobicity

index (HI) was calculated as the aryl C + alkyl C to carboxyl C + O-alkyl C ratio according to Abelmann et al. (2005), and the decomposition index (DI) of SOM was assessed by the alkyl C to O-alkyl C ratio according to Leifeld and Kögel-Knabner (2005). Overall, higher values of ArI, HI and DI indicate higher aromaticity, hydrophobicity and decomposition degree of SOM, respectively.

2.2.2.2. Thermogravimetry (TG) analysis. The TG analyses were conducted in a Discovery SDT 650-Simultaneous TG-DSC instrument (TA Instruments, New Castle, Delaware, USA). For the analysis, 5 mg of dried and finely ground soil (individual replicates) were placed in Alumina crucibles, which were weighed beforehand. The crucibles were then exposed to a N_2 flux, with a flow rate of 50 mL min^{-1}, reduced to 10 mL min^{-1} at the micro-furnace, while being heated and scanned at a constant rate of 20 °C min^{-1}. The temperature range for the scans was from 50 to 900 °C. The area of the thermo-gravimetric curve was divided into five regions (0 to 4) to inform the weight loss according to the degree of resistance of SOM to thermal oxidation (W0: 50–105 °C, water; W1: 105–175 °C, water and very labile organic matter; W2: 175–375 °C, intermediate organic matter; W3: 375–650 °C, recalcitrant organic matter; and W4: 650–850 °C, stable organic matter and minerals) (De la Rosa et al., 2023). The TG curves and weight loss were obtained using the software TRIOS (TA Instruments, New Castle, DE, USA).

The TG index (TGI) of SOM, adapted from Ortner et al. (2025), was calculated as the relative weight loss in W3 (375–650 °C) divided by the relative weight loss in W2 (175–375 °C), assuming a thermal decomposition of major organic constituents between 175 and 650 °C, as similarly performed by Lopez-Capel et al. (2005).

2.2.2.3. Lipid profile. Lipid extraction was performed in duplicate using a batch procedure adapted from Metherel et al. (2009). A 2 g aliquot of each sample was weighed into glass centrifuge tubes, and 15 ml of *n*-hexane was added. The samples were ultrasonicated for 15 min to enhance extraction. Afterwards, the samples were centrifuged for 10 min at 3000 rpm using a Consul 22 centrifuge with an RT 285 rotor (Ortoalresa, Madrid, Spain). The supernatant was collected in a flask, and the sample was re-extracted with an additional 15 ml of *n*-hexane. This procedure was repeated three times to ensure maximum recovery.

The collected extract was concentrated to approximately 1 ml using a rotary evaporator EVA180-B (Labbox Labware, S.L., Premia de Dalt, Barcelona). The extract was then transferred to a chromatography vial, dried to completion, and re-dissolved in 1 ml of *n*-hexane for chromatographic analysis.

A 2 µl aliquot of the lipid extract was injected into a gas chromatograph 7820A (Agilent Technologies, Santa Clara, United States) equipped with an Agilent HP-5MS column (30 m length, 0.25 mm internal diameter, and 0.25 µm film thickness) and an Agilent MS 5973i mass spectrometer (Agilent Technologies, Santa Clara, United States). Helium was used as the carrier gas at a constant flow rate of 1 ml min^{-1}. The temperature program consisted of the following steps: initial temperature of 50 °C for 1 min, a ramp of 30 °C min^{-1} up to 100 °C, a subsequent ramp of 10 °C min^{-1} up to 300 °C and a final isothermal hold at 30 min.

The abundance of compounds was obtained using single ion monitoring traces on a semi-quantitative basis. The relative abundance (%) of each peak within each series was calculated and the peaks grouped in the major compound classes: fatty acids, N-compounds, linear alkanes (high molecular weight), linear alkanes (low molecular weight), S-compounds, other alkanes. The data was expressed as percentage of total ion chromatogram.

Lipid molecular proxies were calculated to assess the contribution of plant and microbial compounds to SOM composition: average chain length (ACL) described as $[(\Sigma zn \times n)/\Sigma zn]$, where zn is the relative amount of the *n*-alkane with *n*-carbons; and C preference index (CPI), which informs about the predominance of odd-over-even in alkane chains ($\Sigma codd/\Sigma ceven$) (Wiesenberg et al., 2010). High values of ACL and CPI are associated with predominant contribution of plant biomass to SOM because of the selective preservation of long chain lipids (Eglinton and Hamilton, 1967).

2.3. Statistical analysis

The data was normally distributed according to Shapiro-Wilk's test and exhibited variance homogeneity according to Levene's test. Thus, the data was subjected to analysis of variance (ANOVA) followed by Tukey's test ($p < 0.05$) to compare means of responsible variables obtained in the different investigated sites within each soil layer. Principal component analysis (PCA) was performed with ^{13}C NMR, TG (except for the 50–105 °C region, because it is attributed to water and not to SOM loss), CPI and ACL data to display shifts in SOM chemical composition at 0–10 and 10–20 cm layers in response to land use change. Because output data of these analyses is expressed on different scales, the z-transformation of the data was conducted before PCA. The quadrants of the PCA biplot were identified as Q1, Q2, Q3 and Q4 to assist results and discussion.

3. Results and discussion

3.1. SOC and TN stocks

The SOC stocks in the 0–10 cm layer varied between 30.6 (Fo + Ba) and 38.6 Mg ha^{-1} (Ba) without significant differences among the sites (Fig. 1a). Similarly, the SOC stocks in the 10–20 cm layer ranged from 16.1 (Fo) to 20.0 Mg ha^{-1} (Ba), without significant differences (Fig. 1a).

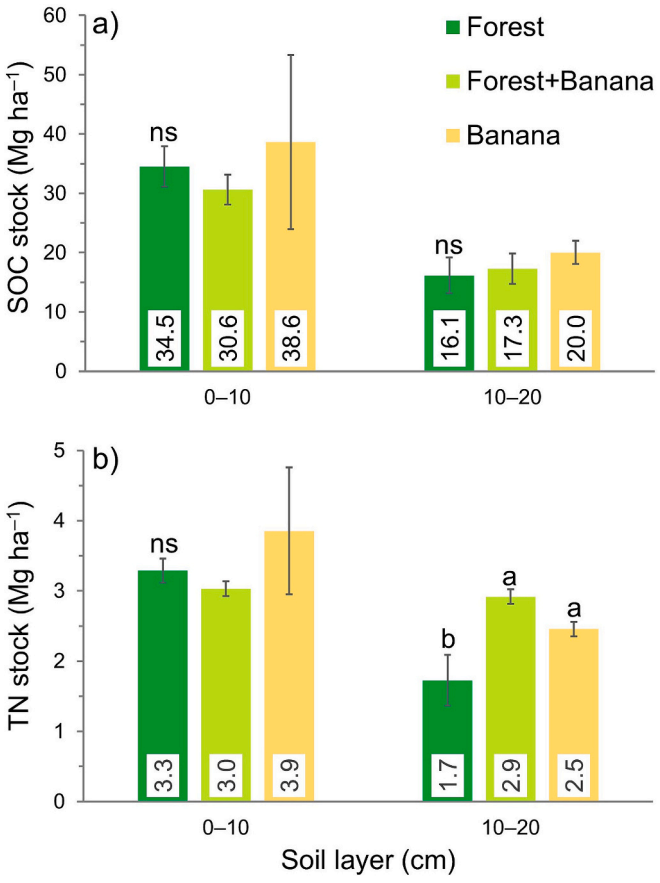

Fig. 1. Total soil organic carbon (SOC) stocks (a) and soil total nitrogen (TN) stocks (b) in the 0–10 and 10–20 cm layer of a Nitisol under Forest, Forest + Banana and Banana. Means followed by different letters within the respective soil layer differ statistically according to Tukey's test ($p < 0.05$). ns = not significant. Error bars show standard deviation.

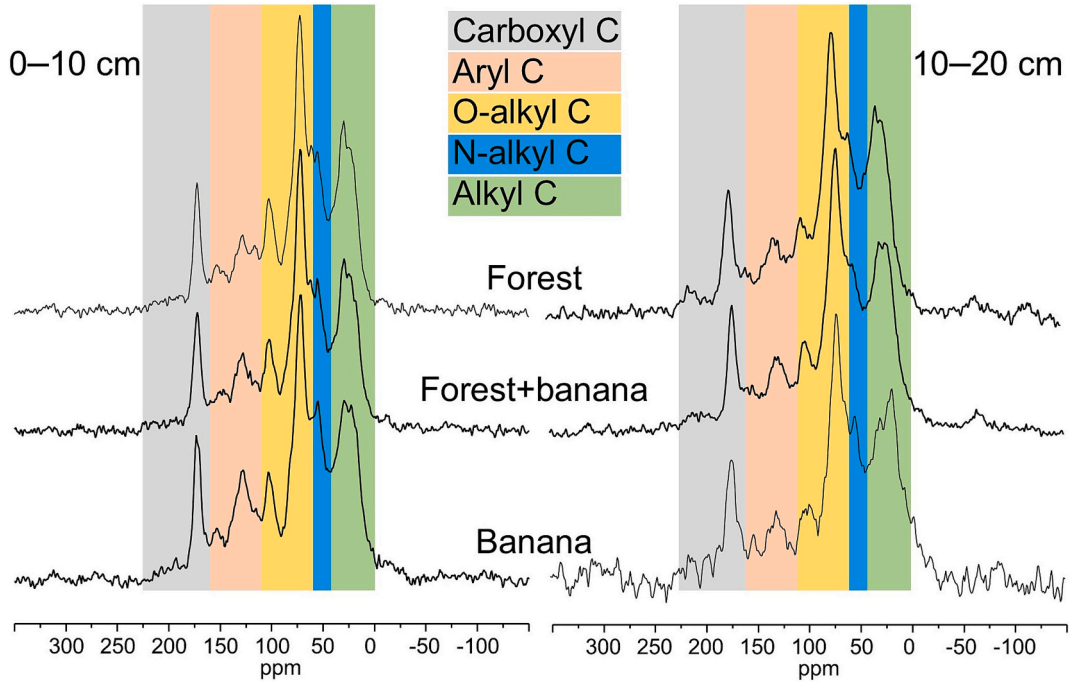

Fig. 2. ^{13}C NMR spectra of soil samples collected in the 0–10 and 10–20 cm layer of a Nitisol under Forest, Forest + Banana and Banana. Spectra regions: 160–225 ppm = carboxyl C, 110–160 ppm = aryl C, 60–110 ppm = O-alkyl C, 45–60 ppm = N-alkyl C, 0–45 ppm = alkyl C.

Overall, these results contradict our first hypothesis. Interestingly, these unchanged SOC stocks contrast with the meta-analysis study by Villela et al. (2026), which reported average SOC stock debits of 7.6 Mg ha^{-1} in the 0–20 cm layer of diverse agricultural systems (from monocropping to integrated systems) formerly under Atlantic Forest. These results suggest that banana systems may have greater capacity to maintain or recover SOC stocks. However, this interpretation should be confirmed by data from a larger number of banana sites.

After 18 years of conversion of Atlantic Forest to Fo + Ba and Ba, it was expected that the lower biomass input to soil specially in Ba system compared to Fo could result in lower SOC stocks. However, our data contradicted such expectations, at least within the examined depth and time after conversion. These results agree with Quartucci et al. (2023) who observed that a 19-year agroforestry system in southeastern Brazil, established after conversion of Atlantic Forest, resulted in a lower addition of biomass C to the soil. The authors also observed no decrease in SOC stock in the 0–40 cm and 0–300 cm layers compared to a secondary Atlantic Forest. These findings disagree also with Silva et al. (2022) who found that the SOC stock (0–20 cm) was reduced by 31.3 Mg ha^{-1} after 30 years of Atlantic Forest conversion to banana cultivation in southeastern Brazil. Together, these findings highlight the need to monitor potential SOC losses in our examined cultivation systems over a longer term, especially because the SOC dynamics in subtropical organic banana agroforestry systems is yet poorly understood.

In general, our findings suggest a remarkable resilience of SOC stocks to land-use change, possibly due to the relatively high clay content of the soils (Table 1), which is known to protect SOC from rapid decomposition (Schweizer et al., 2021; Yang et al., 2021). In general, converting our average (0–20 cm) SOC content (%) data (not shown) obtained by dry combustion to equivalent contents as obtained by sulfochromic oxidation with external heating (regional standard method, 130 °C for 0.5 h) by a factor of 0.98 used for Brazilian soils and then to SOM content by multiplication with 1.724 (Fernandes et al., 2015), the SOM contents of Fo, Fo + Ba and Ba (3.9 to 5.0%) are classified as "intermediate" (2.6–5.0%) according to regional thresholds (CQFS, 2016). In the study region, the SOM class is used to calculate the banana N-fertilization rate. This means that Fo + Ba and Ba may receive the same amount of nitrogen (CQFS, 2016). Although all sites exhibited intermediate SOM content and comparable SOC stocks (0–20 cm), Quartucci et al. (2023) reported significant differences when broader C pools were considered. These authors observed that when accounting for aboveground (living + necromass) and belowground C storage (roots + SOC up to 3 m depth), the C stock in a subtropical secondary Atlantic Forest site (384.3 Mg ha^{-1}) was 134% higher compared to a site with over 25 years of agricultural use, and statistically similar to a site with 19 years of agroforestry. For the cultivated systems of our study (Fo + Ba and Ba), such broader C stock (aboveground + deep-belowground) balance in relation to the Fo reference deserves quantification in future studies.

Soil TN stocks in the 0–10 cm layer varied from 3.3 to 3.9 Mg ha^{-1}, without significant differences among sites (Fig. 1b). However, the TN stock in the 10–20 cm layer of Fo (1.7 Mg ha^{-1}) was 41% and 32% lower than at the Fo + Ba and Ba site, respectively (Fig. 1b). These differences likely resulted from external N additions in the cultivated areas (Fo + Ba and Ba), either in the form of organic amendments (Fo + Ba) or as mineral fertilizer (Ba). Although not significant, the TN at the Ba site tended to be the highest also at 0–10 cm (Fig. 1b), supporting the interpretation of a probable fertilizer contribution. The higher TN stocks may have helped to maintain the SOC stocks in the cultivated systems comparable to that of Fo, as N has been shown to be fundamental for SOC stabilization via organo-mineral interactions (Cotrufo et al., 2019). This is coherent with the lower C:N ratio found in the cultivated systems (5.9–10.1) compared to the forest site (9.4–10.5), irrespective of soil layer. Likely, the higher TN stocks in banana systems stimulated microbial activity and enhanced the decomposition of SOM, promoting the stabilization of decomposed plant material, microbial necromass and bioproducts through association with soil minerals (Manzoni and Cotrufo, 2024). Consequently, the SOM in the cultivated systems appears to be relatively more stabilized, as supported by its enhanced aromaticity and thermal stability (see section 3.2). Additionally, this may also reflect the lower addition of fresh biomass usually found in banana soils compared to forest soil (Quartucci et al., 2023).

Table 2
Relative contribution (%) of carbon chemical groups to the total intensity of ^{13}C NMR spectra, aromaticity index (ArI), hydrophobicity index (HI) and decomposition index (DI) of organic matter of soil samples collected in the 0–10 and 10–20 cm layer of a Nitisol under Forest (Fo), Forest + Banana (Fo + Ba) and Banana (Ba).

		225–160	160–110	110–60	60–45	45–0 ppm			
Site	Layer cm	Carboxyl C %	Aryl C	O-alkyl C	N-alkyl C	Alkyl C	ArI*	HI**	DI***
Fo	0–10	9.9	14.3	37.8	11.2	26.8	0.53	0.86	0.71
Fo + Ba	0–10	11.5	15.0	35.8	10.7	27.0	0.56	0.89	0.75
Ba	0–10	11.7	17.3	33.0	11.0	27.1	0.64	0.99	0.82
Fo	10–20	11.8	12.8	35.0	11.2	29.3	0.44	0.90	0.84
Fo + Ba	10–20	12.1	13.4	34.1	11.0	29.5	0.45	0.93	0.87
Ba	10–20	12.9	11.0	32.9	11.1	32.2	0.34	0.95	0.98

* Aromaticity index (ArI) = aryl C/alkyl C.
** Hydrophobicity index (HI) = (aryl C + alkyl C)/(carboxyl C + O-alkyl C).
*** Decomposition index (DI) = alkyl C/O-alkyl C.

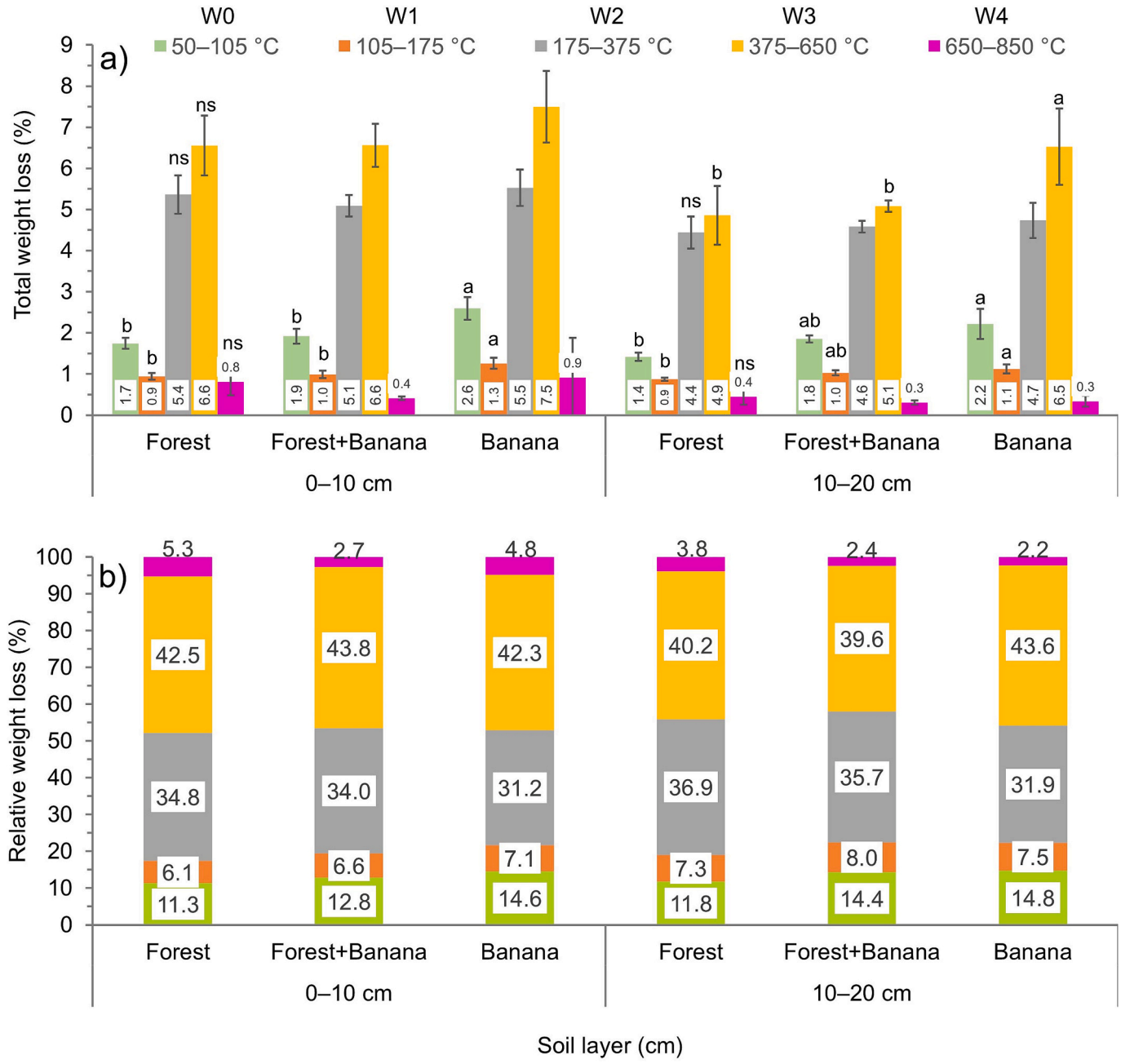

Fig. 3. Total weight loss (a) and relative weight loss (b) in the temperature intervals assessed by thermogravimetry in the 0–10 and 10–20 cm layer of a Nitisol under Forest, Forest + Banana and Banana. Means followed by different letters within a soil layer and temperature interval indicate significant differences according to Tukey's test ($p < 0.05$), ns = not significant. W0, W1, W2, W3 and W4 refer to weight loss in the different temperature ranges. Error bars show standard deviation.

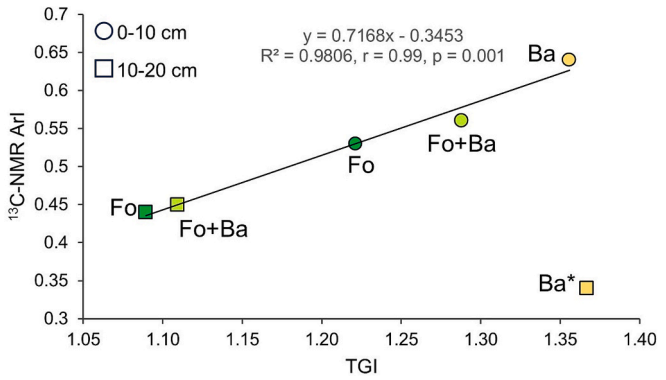

Fig. 4. Relationship between the SOM aromaticity index (ArI), obtained by ^{13}C NMR, and the thermogravimetric index (TGI), obtained by thermal stability analysis of SOM, of soil samples collected in the 0–10 and 10–20 cm layer of a Nitisol under Forest (Fo), Forest + Banana (Fo + Ba) and Banana (Ba). *Excluded from analysis because it was shown that increased thermostability in Banana (10–20 cm) was more strongly relate to enrichment with alkyl C, and less with aryl C.

3.2. *Shifts in SOM structure, thermal stability and lipid proxies*

The analyses of SOM by spectroscopic, thermal and chromatographic techniques revealed clear shifts in SOM composition after land-use change, confirming the interpretations previously inferred from changes in C:N ratios.

3.2.1. *^{13}C NMR and TG analyses*

Overall, the ^{13}C NMR spectra (Fig. 2) exhibited a similar pattern and were dominated by O-alkyl C (32.9 to 37.8%) and by alkyl C signal (26.8 to 32.2%), regardless of site and soil layer (Table 2). The carboxyl C signal was similar across sites both in the 0–10 cm (9.9 to 11.7%) and 10–20 cm (11.8 to 12.9%) layer (Table 2). The sites also exhibited quite similar N-alkyl C signal intensity at 0–10 cm (10.7 to 11.2%) and 10–20 cm (11.0 to 11.2%) layer (Table 2).

The ^{13}C NMR analysis revealed a gradual reduction in O-alkyl C content with land use change intensity (from Fo to Ba) in both layers (Table 2), indicating depletion of labile carbohydrate-rich compounds. This occurred mostly at expenses of increased alkyl C, aryl C, and carboxyl C, in Fo + Ba and Ba (except aryl C in Ba at 10–20 cm) (Table 2). These C-groups are generally associated with more recalcitrant or microbially processed organic matter (Dieckow et al., 2005; Knicker et al., 2012). These trends were reflected in the ArI, HI and DI which tended to increase with land-use intensity (Table 2), indicating a progressive enrichment of SOM with more chemically resistant and hydrophobic components.

The ^{13}C NMR results were well aligned with the TG data (Fig. 3a-b). The TG curves and relative weight loss data are displayed in Fig. S2–S4. In both soil layers, the total weight loss in W3 (recalcitrant SOM), W2 (intermediate SOM), W1 (labile SOM) and W0 (water) tended to decrease in the order Ba > Fo + Ba > Fo (Fig. 3a). However, significant differences in the 0–10 layer occurred only for W0 and W1 (Ba > Fo + Ba = Fo). In the 10–20 cm layer, significant differences occurred for W3 (Ba > Fo + Ba = Fo), W1 and W0 (Ba > Fo, Fo + Ba did not differ from both) (Fig. 3a). Overall, the higher weight loss in W3 of Ba compared to the other sites indicates a greater and preferential accumulation of thermally stable SOM, likely aromatic-C structures (Stoner et al., 2023). Conversely, the higher weight loss in W2 observed for the Fo site is consistent with less altered and more diverse organic inputs from natural litterfall (Gao et al., 2015).

Notably, the TGI correlated strongly with the ArI of ^{13}C NMR as similarly observed in other studies (De la Rosa et al., 2008; Merino et al., 2014; Stoner et al., 2023), but SOM in Ba site at 10–20 cm layer seems to follow a distinct dynamic (Fig. 4). These results indicate that gains in SOM thermal stability in the 10–20 cm layer at the Ba site may be less associated with aromatic condensed-like structures, but more likely with the relative enrichment of stable-hydrophobic alkyl C compounds (Lorenz and Lal, 2009; Bonanomi et al., 2013), which are typical of humified material and lipids in soil (Knicker, 2011; Knicker et al., 2013). In our study, this is supported by a low CPI value, revealing a remarkable enrichment of the 10–20 cm layer of Ba with relatively more degraded *n*-alkanes compared to the other sites (see section 3.2.2). For instance,

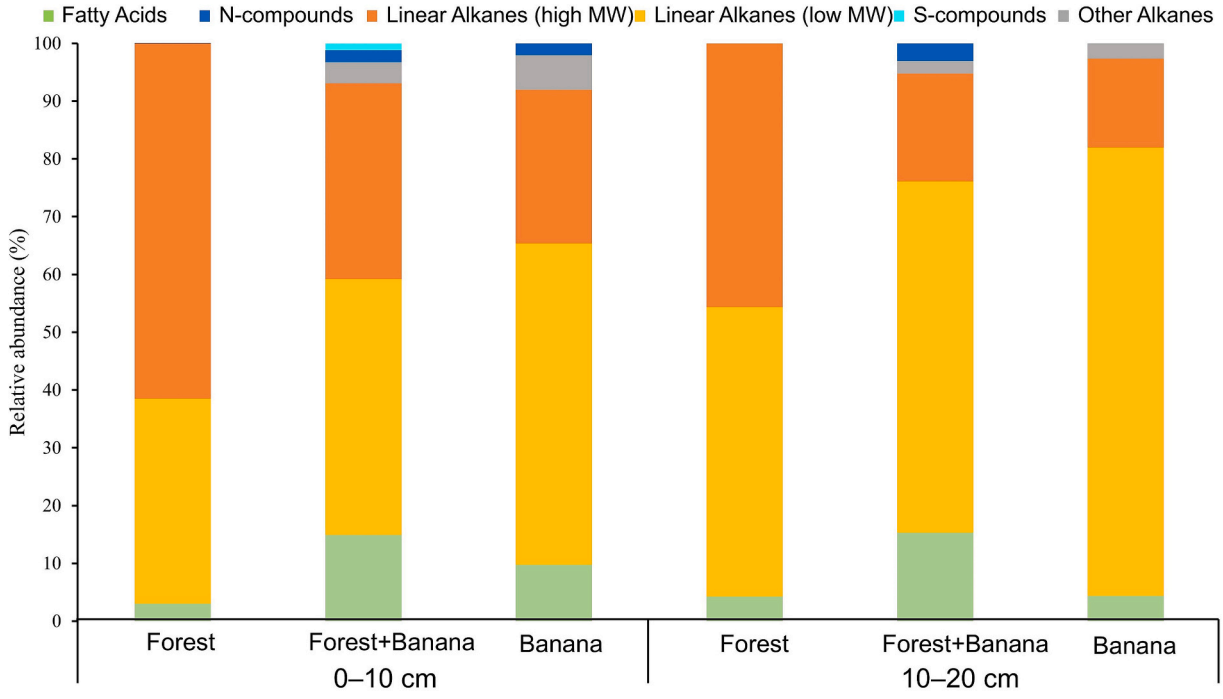

Fig. 5. Relative abundance (%) of major lipid compound classes identified in the free lipid fraction of soil samples collected in the 0–10 and 10–20 cm layer of a Nitisol under Forest, Forest + Banana and Banana.

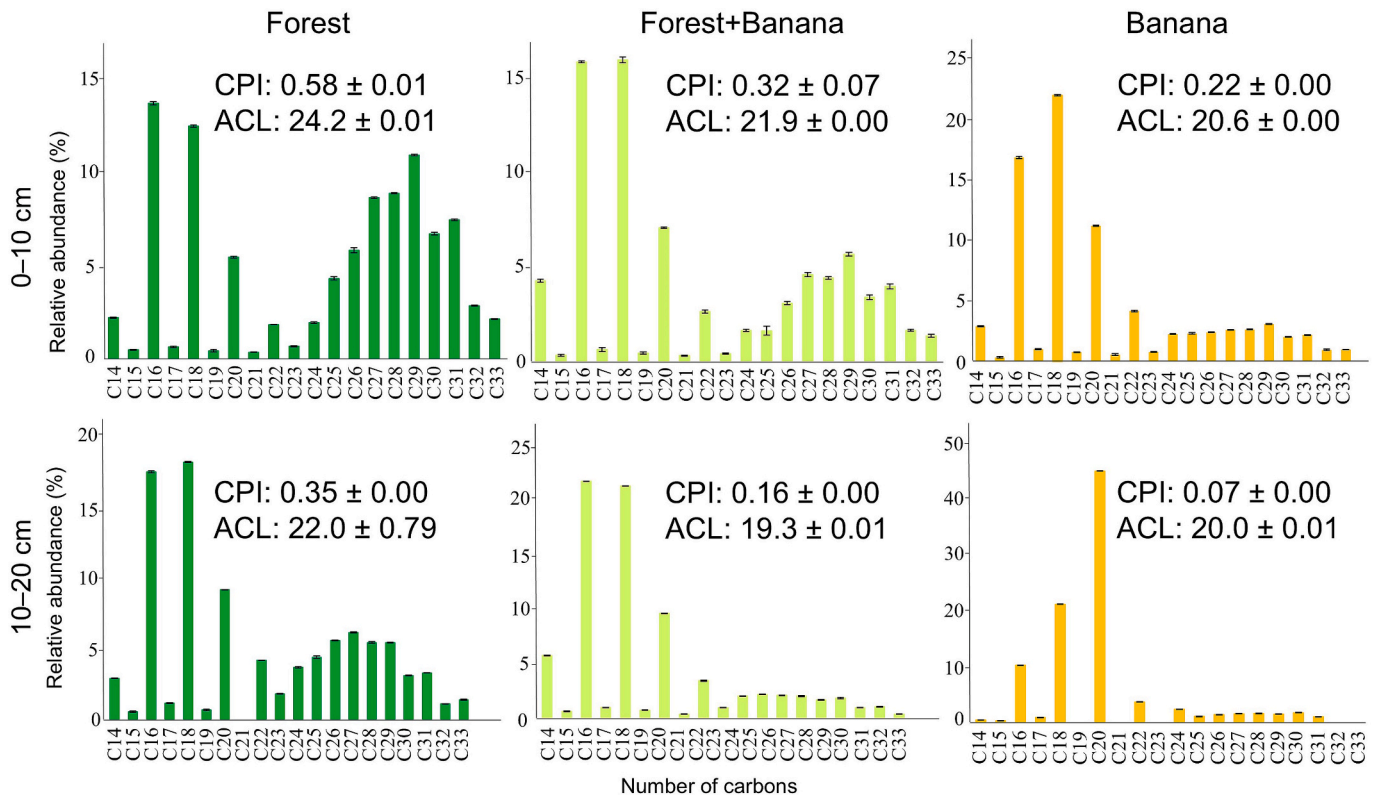

Fig. 6. Distribution of individual *n*-alkanes (C14–C33) in the free lipid fraction of soil samples collected in the 0–10 and 10–20 cm layer of a Nitisol under Forest, Forest + Banana and Banana. CPI = carbon preference index, ACL = average chain length. Error bars show standard deviation. CPI and ACL numbers displayed on the graphs are average followed by ± standard deviation.

Kiem et al. (2000) observed in six long-term field experiments, covering a range of climate features and soil types, a relative enrichment of alkyl C as indicative of a higher degree of SOM decomposition in cultivated soils without organic amendments compared to their pairs receiving fresh organic amendments. This is consistent with the DI, HI and TGI values (Ba > Fo + Ba > Fo) in our study indicating enhanced SOM decomposition, hydrophobicity and thermal stability in response to the intensity of land-use change (Table 2, Fig. 4), regardless of soil layer. This is attributed to conventional agricultural practices, such as those in Ba, which typically result in the depletion of O-alkyl C and other thermally labile compounds, as well as an increased proportion of stable and decomposed C structures in soil (Leifeld et al., 2006; Leifeld et al., 2017).

3.2.2. *Free-lipid analysis*

The analysis of free lipids extracted from soil samples (Fig. 5; Table S2) revealed six major families of organic compounds: *n*-fatty acids, long chain *n*-alkanes, short chain *n*-alkanes, N-containing organic compounds (N-compounds), sulfur-containing compounds (S-compounds), and branched alkanes (other alkanes). Their relative abundance varied across soil layers and land use (Fig. 5). The presence of fatty acids and N-compounds was higher in Fo + Ba, especially at a depth of 10–20 cm (Fig. 5). Minor contributions from S-compounds and other alkane-type compounds were observed across all samples, with no consistent trend (Fig. 5). Interestingly, branched *n*-alkanes were found in the Ba and Fo + Ba soils, but not in the Fo soil (Fig. 5).

In both layers of the Fo soil, the predominant compounds were high molecular weight (MW) linear alkanes (Fig. 5), which are typically associated with undecomposed plant waxes, indicating fresh plant-derived organic matter input (Jiménez-Morillo et al., 2022). In contrast, a higher proportion of low MW linear alkanes and a relative depletion of high MW compounds was found in Ba soil (Fig. 5). Soils under the Fo + Ba system displayed a transitional profile, with more balanced contributions from both high and low MW alkanes (Fig. 5). This was supported by the ACL proxy values, which tended to decrease (Fo > Fo + Ba > Ba) with the increase of land-use intensity (Fig. 6) and agreed with the DI of ^{13}C NMR (Table 2) and the TGI (Fig. 4). Altogether, these results indicate that decomposition degree and thermal stability of SOM increased with land-use change intensity.

The molecular composition of free soil lipids revealed important shifts in both the organic matter sources and the transformation pathways of SOM in response to land-use change. High CPI values typically reflect fresh plant inputs with an odd-over-even predominance of *n*-alkanes, while lower values indicate microbial reworking or more advanced degradation of organic materials (Jansen and Wiesenberg, 2017; Thomas et al., 2021). Similarly, ACL reflects changes in vegetation types and/or climate regimes. Because land-use change alters vegetation cover, microbial activity and litter inputs, both CPI and ACL serve as sensitive molecular indicators of SOM quality under different management systems.

Overall, the CPI and ACL values were highest at the Fo site, confirming the dominant contribution of higher-plant derived alkanes with less microbial alteration. In contrast, Ba soil exhibited markedly lower CPI and ACL values (Fig. 6), reflecting a depletion of long-chain odd-numbered alkanes and a predominance of shorter-chain homologues. This pattern is consistent with intensified microbial processing and selective degradation of plant-derived compounds (Santana et al., 2015). The Fo + Ba system displayed intermediate values, suggesting partial retention of native SOM features under agroforestry, meeting our second hypothesis, at least up to 18 years of the Fo + Ba system.

The composition of soil lipids provided further evidence of these changes. In Fo soils, a broader diversity of lipid classes was detected, including long-chain fatty acids and high MW *n*-alkanes, typically derived from leaf waxes and microbial residues (Table S2). In contrast, Ba soils exhibited a higher relative abundance of short-chain alkanes

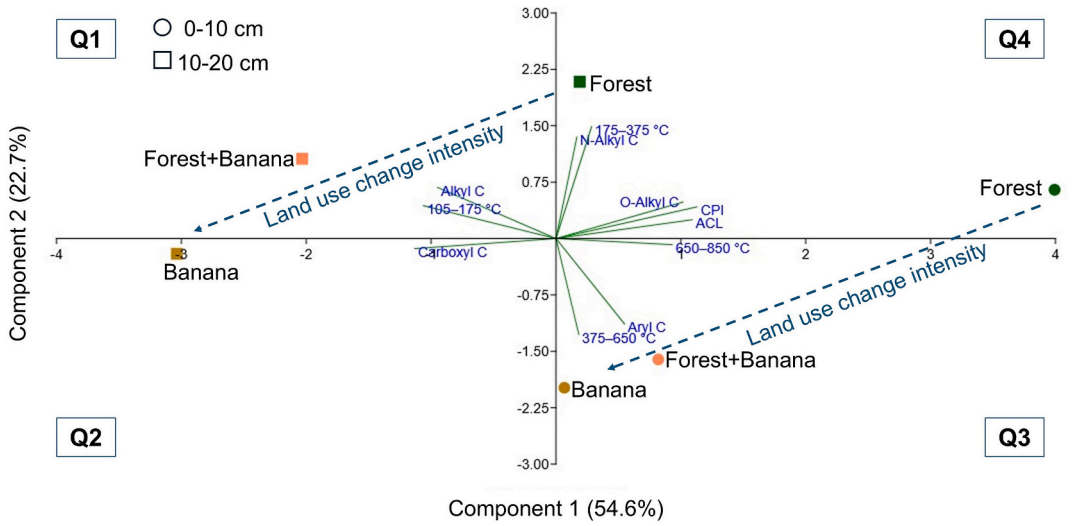

Fig. 7. Principal component analysis biplot of shifts in SOM chemical composition in the 0–10 cm (circles) and 10–20 cm layer (squares) associated with land-use change as revealed by ^{13}C NMR spectra (carboxyl C, aryl C, O-alkyl C, N-alkyl C, alkyl C), TG analysis (105–175 °C = water and very labile organic matter; 175–375 °C = intermediate organic matter; 375–650 °C = recalcitrant organic matter; 650–850 °C = stable organic matter and minerals), and lipid proxies (ACL = average chain length, CPI = carbon preference index). The Q1, Q2, Q3 and Q4 refer to the four PCA quadrants to facilitate discussion of the results. Dashed arrows show the direction of shifts in SOM composition with land use change intensity for each soil layer.

(C15–C20) and N-containing compounds, which are often associated with microbial necromass and more processed SOM (De la Rosa et al., 2008, 2023; Prats et al., 2021). The presence of branched *n*-alkanes solely at the Ba and Fo + Ba soils confirms this finding. This family is typically present in highly microbially degraded SOM (Santana et al., 2015). These results suggest that microbial inputs and decomposition products dominate the lipid pool in intensively managed soils.

Notably, the *n*-alkane distribution in Ba soil showed a clear shift toward lower chain lengths (Fig. 6), further indicating an extensive degradation of the SOM. This observation is in line with the increased abundance of alkyl-C compounds detected in the ^{13}C NMR spectra and supports the notion of selective preservation of microbially derived, alkyl-rich compounds under more intensive land use (Knicker, 2011). This was further confirmed by TG analysis, which revealed increased thermal stability of SOM in Ba soils, associated with a more processed and less labile organic matter pool, as indicated by an increase in W3 at the expense of W1 (De la Rosa et al., 2008; Prats et al., 2021).

The intermediate profile of the Fo + Ba site underscores the potential of agroforestry to buffer SOM degradation, maintaining inputs of higher-plant-derived compounds, while still experiencing enhanced microbial transformation. Altogether, these findings highlight the diagnostic value of lipid biomarkers in tracing SOM quality and suggest that conversion of Atlantic Forest to organic agroforestry and conventional banana systems leads to compositional simplification of SOM.

3.2.3. Comprehensive assessment of SOM composition by PCA analysis

The principal components 1 (PC1) and 2 (PC2) of the PCA biplot explained 54.6% and 22.7%, respectively, of the shifts in SOM composition associated with land-use change (Fig. 7). Notably, the Fo samples collected from the 0–10 cm and 10–20 cm layer plotted within the same quadrant (Q4), suggesting a homogeneous continuum of SOM in this undisturbed system.

In PCA plot, Fo (0–10 cm layer) was ordinated within Q4, mostly due to higher O-alkyl C intensity, ACL and CPI values (Fig. 7). In contrast, Fo + Ba and Ba samples (0–10 cm layer) were ordinated closely together in Q3 in view of their greater aryl C intensity and thermal stability associated with recalcitrant SOM (weight loss in 375–650 °C) (Fig. 7). The 10–20 cm samples of the different sites exhibited a salient dispersion across Q4 (Fo), Q1 (Fo + Ba) and Q2 (Ba) (Fig. 7). This pattern of relative loss of O-alkyl C accompanied by increased alkyl C intensity indicates progressive decomposition degree of SOM with land-use intensity (Fig. 7), as suggested also by the DI (Table 2). Notably, the exclusive presence of Ba (10–20 cm) in Q2, contrary to CPI and ACL in Q4, emphasizes the unique characteristics of SOM in this sample, which is enriched with recalcitrant lipids.

4. Conclusions

We found that after 18 years of Atlantic Forest conversion, the banana systems did not alter significantly the SOC and TN stocks (0–10 cm, 10–20 cm) compared to the reference Atlantic Forest site. Nevertheless, we recommend continued monitoring in similar systems and expanding analyses to include above- and belowground C stocks (at greater depths) to assess potentially negative C balances of banana systems in relation to Atlantic Forest.

Differently from unchanged C stocks, such land use change induced marked shifts in the molecular composition and thermal stability of SOM. Solid-state ^{13}C NMR spectroscopy and TG analyses indicated that land use intensity (Ba > Fo + Ba > Fo) promoted a gradual loss of labile compounds (as O-alkyl C) and enrichment of SOM with more stable structures (alkyl, aryl, and carboxyl C). Consequently, SOM aromaticity, hydrophobicity, and degree of decomposition increased with land-use. Soil lipid proxies support this trend by revealing a relative predominance of lipids of microbial origin in Ba sites. The organic banana agroforestry system partially maintained forest-like SOM features even after nearly two decades of land use change. These findings emphasize that while topsoil C stocks may appear stable after such land use change, the underlying chemical composition of SOM and, thus, its ecological function and long-term stability can be substantially altered.

CRediT authorship contribution statement

Otávio dos Anjos Leal: Writing – review & editing, Writing – original draft, Visualization, Supervision, Methodology, Investigation, Funding acquisition, Formal analysis, Data curation, Conceptualization. **José María De la Rosa:** Writing – original draft, Visualization, Methodology, Formal analysis, Data curation. **Nicolas Brüggemann:** Writing – review & editing, Methodology, Investigation, Funding acquisition. **Holger Wissel:** Methodology, Formal analysis, Data curation. **Cledimar Rogério Lourenzi:** Methodology, Formal analysis, Data curation.

Thairine Evaldt Justo: Methodology, Investigation, Formal analysis, Data curation. **Águeda Sánchez-Martín:** Visualization, Methodology, Investigation, Formal analysis, Data curation. **Deborah Dick:** Supervision, Methodology, Investigation, Conceptualization. **José Antônio González-Pérez:** Writing – review & editing, Supervision, Methodology, Investigation, Formal analysis. **Heike Knicker:** Writing – review & editing, Supervision, Methodology, Investigation, Formal analysis.

Declaration of competing interest

The authors declare that they have no known competing financial interests or personal relationships that could have appeared to influence the work reported in this paper.

Acknowledgements

The first author thanks the farmers Marli and José Deoclécio Justo for accessibility to the investigated sites, Rodrigo Sávio Cadorin, Jayle Velho dos Santos and Leonardo Santos Martins for helping with the soil sampling campaign, and the International Humic Substances Society for the Training Awards received (TRA2019–1), which enabled the acquisition of part of the published data (lipid, TG-DSC and ^{13}C NMR analyses). Águeda Sánchez-Martín thanks the Spanish Ministry of Science and Innovation (MCIN) for her contract as Technical Support Personnel (PTA2021-020000-I).

Appendix A. Supplementary data

Supplementary data to this article can be found online at https://doi.org/10.1016/j.geoderma.2026.117836.

Data availability

Data will be made available on request.

References

Abelmann, K., Kleineidam, S., Knicker, H., Grathwohl, P., Kögel-Knabner, I., 2005. Sorption of HOC in soils with carbonaceous contamination: influence of organic-matter composition. J. Plant Nutr. Soil Sci. 168, 293–306. https://doi.org/10.1002/jpln.200421622.

Almendros, G., González-Pérez, J.A., 2025. Soil organic carbon sequestration mechanisms and the chemical nature of soil organic matter—A review. Sustainability 17 (15), 6689. https://doi.org/10.3390/su17156689.

Alvares, C.A., Stape, J.L., Sentelhas, P.C., Gonçalves, J.L.M., Sparovek, G., 2013. Köppen's climate classification map for Brazil. Meteorol. Z. 22 (6), 711–728. https://doi.org/10.1127/0941-2948/2013/0507.

Beillouin, D., Corbeels, M., Demenois, J., Berre, D., Boyer, A., Fallot, A., Feder, F., Cardinael, R., 2023. A global meta-analysis of soil organic carbon in the Anthropocene. Nat. Commun. 14, 3700. https://doi.org/10.1038/s41467-023-39338-z.

Bernoux, M., Carvalho, M.C.S., Volkoff, B., Cerri, C.C., 2002. Brazil's soil carbon stocks. Soil Sci. Soc. Am. J. 66, 888–896. https://doi.org/10.2136/sssaj2002.8880.

Bieluczyk, W., Asselta, F.O., Navroski, D., Gontijo, J.B., Venturini, A.M., Mendes, L.W., Simon, C.P., Camargo, P.B., Tadini, A.M., Martin-Neto, L., Bendassoli, J.A., Rodrigues, R.R., Putten, W.H., Tsai, S.M., 2023. Linking above and belowground carbon sequestration, soil organic matter properties, and soil health in Brazilian Atlantic Forest restoration. J. Environ. Manage. 344, 118573. https://doi.org/10.1016/j.jenvman.2023.118573.

Bonanomi, G., Incerti, G., Giannino, F., Mingo, A., Lanzotti, V., Mazzoleni, S., 2013. Litter quality assessed by solid-state ^{13}C NMR spectroscopy predicts decay rate better than C/N and lignin/N ratios. Soil Biol. Biochem. 56, 40–48. https://doi.org/10.1016/j.soilbio.2012.03.003.

Carlucci, M.B., Marcilio-Silva, V., Torezan, J.M., 2021. The Southern Atlantic Forest: use, degradation, and perspectives for conservation. In: Marques, M.C.M., Grelle, C.E.V. (Eds.), The Atlantic Forest. Springer, Cham, 10.1007/978-3-030-55322-7_5.

Chukov, S.N., Lodygin, E.D., Abakumov, E.V., 2018. Application of ^{13}C NMR spectroscopy to the study of soil organic matter: a review of publications. Eurasian Soil Sci. 51, 889–900. https://doi.org/10.1134/S1064229318080021.

Cotrufo, M.F., Ranalli, M.G., Haddix, M.L., Six, J., Lugato, E., 2019. Soil carbon storage informed by particulate and mineral-associated organic matter. Nat. Geosci. 12, 898–994. https://doi.org/10.1038/s41561-019-0484-6.

CQFS - Comissão de Química e Fertilidade do Solo. 2016. Manual de adubação e calagem para os estados do Rio Grande do Sul e de Santa Catarina. Ed. SBCS-NRS: Porto Alegre.

De la Rosa, J.M., Knicker, H., 2011. Bioavailability of N released from N-rich pyrogenic organic matter: an incubation study. Soil Biol. Biochem. 43 (12), 2368–2373. https://doi.org/10.1016/j.soilbio.2011.08.008.

De la Rosa, J.M., Knicker, H., López-Capel, E., Maning, D.A.C., González-Pérez, J.A., González-Vila, F.J., 2008. Direct detection of black carbon in soils by Py-GC/MS, Carbon-13 NMR spectroscopy and thermogravimetric techniques. Soil Sci. Soc. Am. J. 72, 258–267. https://doi.org/10.2136/sssaj2007.0031.

De la Rosa, J.M., Miller, A.Z., Knicker, H., 2018. Soil-borne fungi challenge the concept of long-term biochemical recalcitrance of pyrochar. Sci. Rep. 8, 2896. https://doi.org/10.1038/s41598-018-21257-5.

De la Rosa, J.M., Pérez-Dalí, S.M., Campos, P., Sánchez-Martín, Á., González-Pérez, J.A., Miller, A.Z., 2023. Suitability of volcanic ash, rice husk ash, green compost and biochar as amendments for a mediterranean alkaline soil. Agronomy 13 (4), 1097. https://doi.org/10.3390/agronomy13041097.

Dieckow, J., Bayer, C., Conceição, P.C., Zanatta, J.A., Martin-Neto, L., Milori, D.B.M., Salton, J.C., Macedo, M.M., Mielniczuk, J., Hernani, L.C., 2009. Land use, tillage, texture and organic matter stock and composition in tropical and subtropical Brazilian soils. Eur. J. Soil Sci. 60 (2), 240–249. https://doi.org/10.1111/j.1365-2389.2008.01101.x.

Dieckow, J., Mielniczuk, J., Knicker, H., Bayer, C., Dick, D.P., Kögel-Knaber, I., 2005. Composition of organic matter in a subtropical Acrisol as influenced by land use cropping and N fertilization, assessed by CPMAS ^{13}C NMR spectroscopy. Eur. J. Soil Sci. 56, 705–715. https://doi.org/10.1111/j.1365-2389.2005.00705.x.

Eglinton, E., Hamilton, R.J., 1967. Leaf epicuticular waxes. Science 156, 1322–1334. https://doi.org/10.1126/science.156.3780.1322.

FAO, 2009. Global agriculture towards 2050. High-level expert Forum. 2009. Available at: https://www.fao.org/fileadmin/templates/wsfs/docs/Issues_papers/HLEF2050_Global_Agriculture.pdf (Accessed 24 September 2025).

FAO, 2025. Annual Population data. Available at: . (Accessed 24 September 2025).

FAO and ITPS, 2015. Status of the World's Soil Resources (SWSR) – Main Report. Food and Agriculture Organization of the United Nations, Rome, Italy. Available at: https://openknowledge.fao.org/server/api/core/bitstreams/6ec24d75-19bd-4f1f-b1c5-5becf50d0871/content (Accessed 24 September 2025).

Fernandes, R.B.A., Carvalho-Junior, I.A., Ribeiro-Junior, E.S., de Sá Mendonça, E., 2015. Comparison of different methods for the determination of total organic carbon and humic substances in Brazilian soils. Rev. Ceres. 62 (5), 496–501. https://doi.org/10.1590/0034-737X201562050011.

FiBL – Research Institute of Organic Agriculture and IFOAM – Organics International, 2015. The World of Organic Agriculture 2025. Statistics and Emerging Trends 2015. Available at: https://www.fibl.org/fileadmin/documents/shop/1663-organic-world-2015.pdf (Accessed 24 September 2025).

FiBL – Research Institute of Organic Agriculture and IFOAM – Organics International, 2025. The World of Organic Agriculture 2025. Statistics and Emerging Trends 2025. Available at: https://orgprints.org/id/eprint/54617/1/1797-organic-world-2025.pdf (Accessed 24 September 2025).

Freitas, V.S., Babos, D.V., Guedes, W.N., Silva, F.P., Tozo, M.L.L., Andrade, C.A., Villas Boas, P.R., Milori, D.M.B.P., Martin-Neto, L., 2024. Soil organic matter dynamics and soil carbon stocks from tropical and sub-tropical areas under no-till: an on-farm research. Catena. 247, 108491. https://doi.org/10.1016/j.catena.2024.108491.

Gao, W., Zhou, T., Ren, T., 2015. Conversion from conventional to No tillage alters thermal stability of organic matter in soil aggregates. Soil Sci. Soc. Am. J. 79, 213–222. https://doi.org/10.2136/sssaj2014.08.0334.

Gonçalves, A.L., 2008. Ecological agriculture in the Torres region of Rio Grande do Sul, Brazil: Tradeoffs or synergies? Cornell University. PhD Dissertation.

Gonçalves, A.L., Motter, C., 2015. Produção Ecológica de Banana. Available at: https://www.centroecologico.org.br/cartilhas/Cartilha_Banana_CE.pdf (Accessed 24 September 2025).

Gonçalves, C.N., Dalmolin, R.S.D., Dick, D.P., Knicker, H., Klamt, E., Kögel-Knaber, I., 2003. The effect of 10% HF treatment on the resolution of CPMAS ^{13}C NMR spectra and on the quality of organic matter in Ferrasols. Geoderma 116, 373–392. https://doi.org/10.1016/S0016-7061(03)00119-8.

IBGE - Instituto Brasileiro de Geografia e Estatística, 2025. Produção de Banana. Available at: https://www.ibge.gov.br/explica/producao-agropecuaria/banana/br (Accessed 24 September 2025).

IUSS Working Group WRB, 2015. World Soil Resources Reports No. 106: World Reference Base for Soils Resources 2014. Food and Agriculture Organization of the United Nations (FAO), Rome. Available at: https://openknowledge.fao.org/server/api/core/bitstreams/bcdecec7-f45f-4dc5-beb1-97022d29fab4/content (Accessed 24 September 2025).

Jansen, B., Wiesenberg, G.L.B., 2017. Opportunities and limitations related to the application of plant-derived lipid molecular proxies in soil science. Soil. 3, 211–234. https://doi.org/10.5194/soil-3-211-2017.

Jiménez-Morillo, N.T., Almendros, G., Miller, A.Z., Hatcher, P.G., González-Pérez, J.A., 2022. Hydrophobicity of soils affected by fires: an assessment using molecular markers from ultra-high resolution mass spectrometry. Sci. Total Environ. 817, 152957. https://doi.org/10.1016/j.scitotenv.2022.152957.

Kiem, R., Knicker, H., Körschens, M., Kögel-Knabner, I., 2000. Refractory organic carbon in C-depleted arable soils, as studied by ^{13}C NMR spectroscopy and carbohydrate analysis. Org. Geochem. 31 (7–8), 655–668. https://doi.org/10.1016/S0146-6380(00)00047-4.

Knicker, H., 2011. Solid state CPMAS ^{13}C and ^{15}N NMR spectroscopy in organic geochemistry and how spin dynamics can either aggravate or improve spectra interpretation. Org. Geochem. 42 (8), 867–890. https://doi.org/10.1016/j.orggeochem.2011.06.019.

Knicker, H., González-Vila, F.J., González-Vásquez, R., 2013. Biodegradability of organic matter in fire-affected mineral soils of Southern Spain. Soil Biol. Biochem. 56, 31–39. https://doi.org/10.1016/j.soilbio.2012.02.021.

Knicker, H., Nikolova, R., Dick, D.P., Dalmolin, R.S.D., 2012. Alteration of quality and stability of organic matter in grassland soils of Southern Brazil highlands after ceasing biannual burning. Geoderma. 181–182, 11–21. https://doi.org/10.1016/j.geoderma.2012.03.001.

Knicker, H., Totsche, K.U., Almendros, G., González-Vila, F.J., 2005. Condensation degree of burnt peat and plant residues and the reliability of solid-state VACP MAS ^{13}C NMR spectra obtained from pyrogenic humic material. Org. Geochem. 36, 1359–1377. https://doi.org/10.1016/j.orggeochem.2005.06.006.

Leifeld, J., Alewell, C., Bader, C., Krüger, J.P., Mueller, C.W., Sommer, M., Steffens, M., Szidat, S., 2017. Pyrogenic carbon contributes substantially to carbon storage in intact and degraded northern peatlands. Land Degrad. Develop. 29, 2082–2091. https://doi.org/10.1002/ldr.2812.

Leifeld, J., Franko, U., Schulz, E., 2006. Thermal stability responses of soil organic matter to long-term fertilization practices. Biogeosciences. 3 (3), 371–374. https://doi.org/10.5194/bg-3-371-2006.

Leifeld, J., Kögel-Knabner, I., 2005. Soil organic matter fractions as early indicators for carbon stock changes under different land-use? Geoderma 124 (1–2), 143–155. https://doi.org/10.1016/j.geoderma.2004.04.009.

Lopez-Capel, E., Sohi, S.P., Gaunt, J.L., Manning, D.A.C., 2005. Use of thermogravimetry–differential scanning calorimetry to characterize modelable soil organic matter fractions. Soil Sci. Soc. Am. J. 69 (1), 136–140. https://doi.org/10.2136/sssaj2005.0136a.

Lorenz, K., Lal, R., 2009. Stabilization of organic carbon in chemically separated pools in reclaimed coal mine soils in Ohio. Geoderma. 141, 294–301. https://doi.org/10.1016/j.geoderma.2007.06.008.

Manzoni, S., Cotrufo, F., 2024. Mechanisms of soil organic carbon and nitrogen stabilization in mineral associated organic matter – insights from modelling in phase space. Biogeosciences 21, 4077–4098. https://doi.org/10.5194/egusphere-2024-1092.

Metherel, A.H., Taha, A.Y., Izadi, H., Stark, K.D., 2009. The application of ultrasound energy to increase lipid extraction throughput of solid matrix samples (flaxseed). PLEFA 81, 417–423. https://doi.org/10.1016/j.plefa.2009.07.003.

Merino, A., Ferreiro, A., Salgado, J., Fontúrbel, M.T., Barros, N., Fernández, C., Vega, J. A., 2014. Use of thermal analysis and solid-state ^{13}C CP-MAS NMR spectroscopy to diagnose organic matter quality in relation to burn severity in Atlantic soils. Geoderma. 226–227, 376–386. https://doi.org/10.1016/j.geoderma.2014.03.009.

Ortner, M., Seidel, S., Diehl, M., Vohland, D., 2025. Assignment of thermogravimetric mass losses to soil organic matter, its fractions hot water-extractable and microbial biomass carbon, and organic matter-stabilizing soil mineral properties. J. Plant Nutr. Soil Sci. 188, 334–349. https://doi.org/10.1002/jpln.202400498.

Plante, A.F., Fernández, J.M., Leifeld, J., 2009. Application of thermal analysis techniques in soil science. Geoderma. 153, 1–10. https://doi.org/10.1016/j.geoderma.2009.08.016.

Prats, S.A., Merino, A., Gonzalez-Perez, J.A., Verheijen, F.G., De la Rosa, J.M., 2021. Can straw-biochar mulching mitigate erosion of wildfire-degraded soils under extreme rainfall? Sci. Total Environ. 761, 143219. https://doi.org/10.1016/j.scitotenv.2020.143219.

Quartucci, F., Gocke, M., Denich, M., Gonçalves, J.L.M., Amelung, W., 2023. Deep soil carbon loss offsets rapid aboveground carbon accumulation after reforestation. For. Ecol. Manage. 548, 121403. https://doi.org/10.1016/j.foreco.2023.121403.

Ramos, A.P., Lima, S.S., Ferreira, C.S., Pinto, L.A.R., Ferreira, R., Dias, A., Matos, P.S., Pereira, M.G., 2025. Macrofauna and soil properties in agroforestry system and secondary forest. Rev. Bras. Ci. Solo. 49, e0240091. https://doi.org/10.36783/18069657rbcs20240091.

Rezende, C.L., Scarano, F.R., Assad, E.D., Joly, C.A., Metzger, J.P., Strassburg, B.B.N., Tabarelli, M., Fonseca, G.A., Mittermeier, R.A., 2018. From hotspot to hopespot: an opportunity for the Brazilian Atlantic Forest. Perspect. Ecol. Conserv. 16 (4), 208–214. https://doi.org/10.1016/j.pecon.2018.10.002.

Ribeiro, M.C., Metzger, J.P., Martensen, A.C., Ponzoni, F.J., Hirota, M.M., 2009. The Brazilian Atlantic Forest: how much is left, and how is the remaining forest distributed? Implications for conservation. Biol. Conserv. 142 (6), 1141–1153. https://doi.org/10.1016/j.biocon.2009.02.021.

Rossato, D.O., Iserhard, C.A., Nakamura, G., Duarte, L., Nadeau, N., 2025. The effects of agroforestry and conventional banana plantations on multiple dimensions of butterfly diversity in the Atlantic Forest. Biodivers. Conserv. 34 (6), 2401–2424. https://doi.org/10.1007/s10531-025-03075-0.

Sá, J.C.M., Gonçalves, D.R.P., Ferreira, L.A., Mishra, U., Inagaki, T.M., Furlan, F.J.F., Moro, R.S., Floriani, N., Briedis, C., Ferreira, A.O., 2018. Soil carbon fractions and biological activity based indices can be used to study the impact of land management and ecological successions. Ecol. Indic. 84, 96–105. https://doi.org/10.1016/j.ecolind.2017.08.029.

Santana, G.S., Knicker, H., González-Vila, F.J., González-Pérez, J.A., Dick, D.P., 2015. The impact of exotic forest plantations on the chemical composition of soil organic matter in Southern Brazil as assessed by Py–GC/MS and lipid extracts study. Geoderma Reg. 4, 11–19. https://doi.org/10.1016/j.geodrs.2014.11.004.

Santos, H.G., Jacomine, P.K.T., Anjos, L.H.C., Oliveira, V.A., Lumbreras, J.F., Coelho, M. R., 2018. Sistema Brasileiro de Classificação de Solos, fifth ed. Embrapa, Brasília. Available at: https://ainfo.cnptia.embrapa.br/digital/bitstream/item/199517/1/SiBCS-2018-ISBN-9788570358004.pdf.

Santos, C.A., Rezende, C.P., Pinheiro, E.F.M., Pereira, J.M., Alves, B.J.R., Urquiaga, S., Boddey, R.M., 2019. Changes in soil carbon stocks after land-use change from native vegetation to pastures in the Atlantic Forest region of Brazil. Geoderma. 337, 394–401. https://doi.org/10.1016/j.geoderma.2018.09.045.

Schweizer, S.A., Mueller, C.W., Höschen, C., Ivanov, P., Kögel-Knabner, I., 2021. The role of clay content and mineral surface area for soil organic carbon storage in an arable toposequence. Biogeochemistry 156 (3), 401–420. https://doi.org/10.1007/s10533-021-00850-3.

Silva, R.B., Rosa, J.S., Packer, A.P., Bento, C.B., Silva, F.A.M., 2022. A soil quality physical–chemical approach 30 years after land-use change from forest to banana plantation. Environ. Monit. Assess. 194 (7), 482. https://doi.org/10.1007/s10661-022-10167-9.

Stockmann, U., et al., 2013. The knowns, known unknowns and unknowns of sequestration of soil organic carbon. Agr. Ecosyst. Environ. 164, 80–99. https://doi.org/10.1016/j.agee.2012.10.001.

Stoner, S., Trumbore, S.E., González-Pérez, J.A., Schrumpf, M., Sierra, C.A., Hoyt, A.M., Chadwick, O., Doetterl, S., 2023. Relating mineral–organic matter stabilization mechanisms to carbon quality and age distributions using ramped thermal analysis. Philos. Trans. R. Soc. A 381, 20230139. https://doi.org/10.1098/rsta.2023.0139.

Teixeira, C.S., Holland-Moritz, H., Bayer, C., Granada, C.E., Sausen, T.L., Tonial, F., Petry, C., Frey, S.D., 2024. Land management of formerly subtropical Atlantic Forest reduces soil carbon stocks and alters microbial community structure and function. Appl. Soil Ecol. 195, 105252. https://doi.org/10.1016/j.apsoil.2023.105252.

Teixeira, P.C., Donagemma, G.K., Fontana, A., Teixeira, W.G., 2017. Manual de Métodos de Análise de Solo, third ed. Embrapa, Brasília. Available at: https://www.infoteca.cnptia.embrapa.br/handle/doc/1085209.

Thomas, C.L., Jansen, B., van Loon, E.E., Wiesenberg, G.L.B., 2021. Transformation of *n*-alkanes from plant to soil: a review. SOIL. 7, 785–809. https://doi.org/10.5194/soil-7-785-2021.

United Nations, 2013. World population prospects. The 2012 revision. Available at: (Accessed 24 September 2025).

United Nations, 2024. World Population Prospects 2024. Summary of Results. Available at: https://population.un.org/wpp/assets/Files/WPP2024_Summary-of-Results.pdf (Accessed 24 September 2025).

USDA, 2015. Soil quality indicators - Physical, chemical, and biological indicators for soil quality assessment and management. Available at: (Accessed 24 September 2025).

Villela, J.M., Damian, J.M., Gonçalves, D.R.P., Barioni, L.G., Cherubin, M.R., Cerri, E.P., 2026. Soil carbon debt from land use change in Brazil. Nat. Commun. 17, 1626. https://doi.org/10.1038/s41467-026-68340-4.

Wei, X., Shao, M., Gale, W., Li, L., 2014. Global pattern of soil carbon losses due to the conversion of forests to agricultural land. Sci. Rep. 4, 4062. https://doi.org/10.1038/srep04062.

Weidlich, E.W.A., 2025. Brazil's dangerous environmental licensing bill. Science 389 (6760), 583–584. https://doi.org/10.1126/science.aea7981.

Wiesenberg, G.L.B., Dorodnikov, M., Kuzyakov, Y., 2010. Source determination of lipids in bulk soil and soil density fractions after four years of wheat cropping. Geoderma. 156, 267–277. https://doi.org/10.1016/j.geoderma.2010.02.026.

Yang, J.Q., Zhang, X., Bourg, I.C., Stone, H.A., 2021. 4D imaging reveals mechanisms of clay-carbon protection and release. Nat. Commun. 12 (1), 622. https://doi.org/10.1038/s41467-020-20798-6.